$p16^{INK4a}$ reporter mice reveal age-promoting effects of environmental toxicants

Jessica A. Sorrentino, … , Christin E. Burd, Norman E. Sharpless

Brief Report   Aging

While murine-based systems to identify cancer-promoting agents (carcinogens) are established, models to identify compounds that promote aging (gerontogens) have not been described. For this purpose, we exploited the transcription of $p16^{INK4a}$, which rises dynamically with aging and correlates with age-associated disease. Activation of $p16^{INK4a}$ was visualized in vivo using a murine strain that harbors a knockin of the luciferase gene into the *Cdkn2a* locus ($p16^{LUC}$ mice). We exposed $p16^{LUC}$ mice to candidate gerontogens, including arsenic, high-fat diet, UV light, and cigarette smoke and serially imaged animals to monitor senescence induction. We show that exposure to a high-fat diet did not accelerate $p16^{INK4a}$ expression, whereas arsenic modestly augmented, and cigarette smoke and UV light potently augmented, activation of $p16^{INK4a}$-mediated senescence. This work provides a toxicological platform to study mammalian aging and suggests agents that directly damage DNA promote molecular aging.

Find the latest version:

p16^INK4a reporter mice reveal age-promoting effects of environmental toxicants

Jessica A. Sorrentino,[1,2] Janakiraman Krishnamurthy,[2,3] Stephen Tilley,[4]
James G. Alb Jr.,[2,5] Christin E. Burd,[6] and Norman E. Sharpless[1,2,3]

[1]The Curriculum in Toxicology, University of North Carolina at Chapel Hill, Chapel Hill, North Carolina, USA. [2]The Lineberger Comprehensive Cancer Center,
[3]Department of Genetics, and [4]Department of Pulmonary Medicine, University of North Carolina School of Medicine, Chapel Hill, North Carolina, USA.
[5]Department of Cell Biology and Physiology, University of North Carolina at Chapel Hill, Chapel Hill, North Carolina, USA.
[6]Departments of Molecular Genetics and Molecular and Cellular Biochemistry, The Ohio State University, Columbus, Ohio, USA.

While murine-based systems to identify cancer-promoting agents (carcinogens) are established, models to identify compounds that promote aging (gerontogens) have not been described. For this purpose, we exploited the transcription of *p16^INK4a*, which rises dynamically with aging and correlates with age-associated disease. Activation of *p16^INK4a* was visualized in vivo using a murine strain that harbors a knockin of the luciferase gene into the *Cdkn2a* locus (*p16^LUC* mice). We exposed *p16^LUC* mice to candidate gerontogens, including arsenic, high-fat diet, UV light, and cigarette smoke and serially imaged animals to monitor senescence induction. We show that exposure to a high-fat diet did not accelerate *p16^INK4a* expression, whereas arsenic modestly augmented, and cigarette smoke and UV light potently augmented, activation of *p16^INK4a*-mediated senescence. This work provides a toxicological platform to study mammalian aging and suggests agents that directly damage DNA promote molecular aging.

Introduction

Murine models have been critical to the identification of carcinogens. For example, commercially available models (i.e., BigBlue, MutaMouse, and the *p53*^+/– strain; refs. 1–3) represent core tools in cancer toxicology. These reagents increase the efficiency and sensitivity of carcinogen identification, while reducing animal requirements and costs. In 1987, Martin proposed the concept of gerontogens (4): environmental agents that accelerate molecular aging, analogous to carcinogens promoting neoplasia. While murine models for carcinogen testing are advanced, in vivo tools for gerontogen testing do not exist.

Mammalian aging is complex, with distinct molecular processes contributing to age-related tissue dysfunction. While no single process underpins aging, several lines of evidence suggest senescence activation is an important contributor. Markers of cellular senescence dramatically increase with aging in humans and mice, including expression of the *p16^INK4a* tumor suppressor gene (5–8). Moreover, activation of *p16^INK4a* and senescence has been linked to replicative hypofunction in neural stem cells (9), hematopoietic progenitors (10), lymphocytes (11, 12), and pancreatic β cells (13). Altered regulation of the senescence-promoting *CDKN2a/b* locus, which encodes p16^INK4a, p15^INK4b, and ARF, has been linked to aging phenotypes, including atherosclerotic disease, type II diabetes, glaucoma, and several malignancies (14). Finally, pharmacologic and genetic approaches to manipulating the number of senescent cells in vivo can ameliorate age-associated phenotypes such as sarcopenia, kyphosis, and hyporeplication of T lymphocytes and pancreatic β cells (15–17). Here, we sought to determine

whether in vivo activation of *p16^INK4a*, measured using the recently described *p16^LUC* reporter allele (18), could effectively assess the gerontogenic effects of environmental agents.

Results and Discussion

The *p16^LUC* allele features firefly luciferase knocked in to exon 1α of the murine *Cdkn2a* locus (18), with expression under the control of the endogenous *p16^INK4a* promoter and distant *cis*-regulatory elements (19, 20). Importantly, *p16^INK4a* expression is negligible in healthy cells from young mice, but increases more than 300-fold on a per-cell basis with age-promoting stresses (7, 18). The large, dynamic range of *p16^INK4a* expression makes *p16^LUC* a valuable tool for in vivo imaging of senescence induction. To assess the effect of candidate gerontogens — high-fat diet (HFD), UV light, arsenic, and cigarette smoke (CS) — on senescence, we performed serial analysis of *p16^LUC* cohorts.

Prior studies on the effects of obesity and HFD on *p16^INK4a* expression in vivo have yielded inconsistent results. HFD has been reported to increase senescence and/or *p16^INK4a* expression in vascular cells (21, 22), whereas *p16^INK4a* mRNA expression in peripheral blood T lymphocytes (PBTLs) does not correlate with body mass index, a marker of obesity, in humans (8). To examine the effects of HFD on whole-body senescence, littermate *p16^LUC* mice were placed on a 42%-fat HFD or 4%-fat normal diet (ND) for 18 months starting at 8–10 weeks of age. HFD feeding produced a clear pharmacodynamic effect, causing significant weight gain and hepatic steatosis, although no differences in overall survival were noted (Supplemental Figure 1, A–C; supplemental material available online with this article; doi:10.1172/JCI70960DS1). Consistent with prior reports (7, 18), we observed an exponential increase in *p16^INK4a* expression with aging; however, the rate of increase, as assessed by total-body luciferase imaging (TBLI), was not different between cohorts (Figure 1, A and B). Due to the wide range of weight gain among HFD-fed mice, we analyzed the relationship between weight and luciferase intensity at 52 weeks and observed no correlation (Supplemental Figure 1D). Corre-
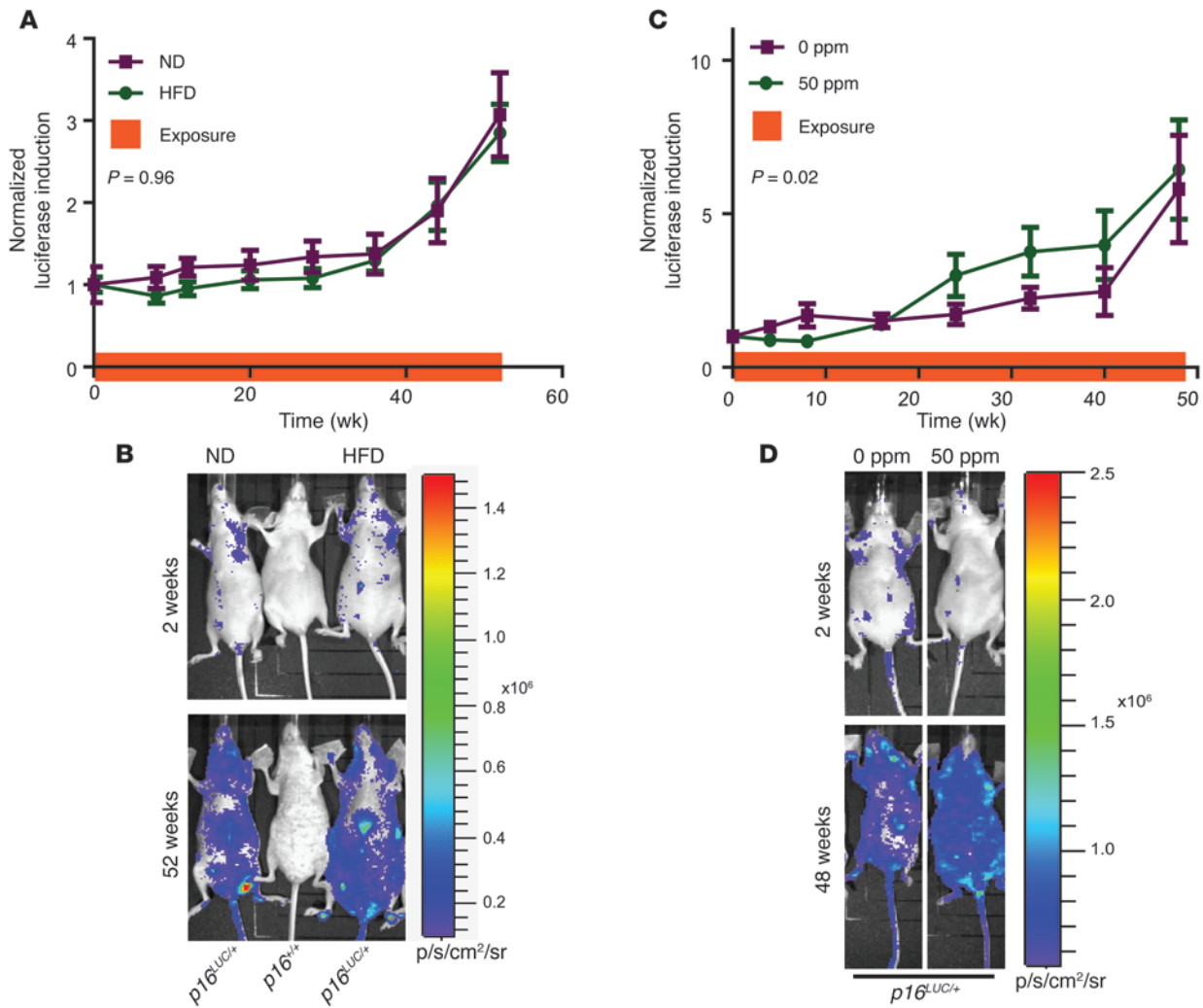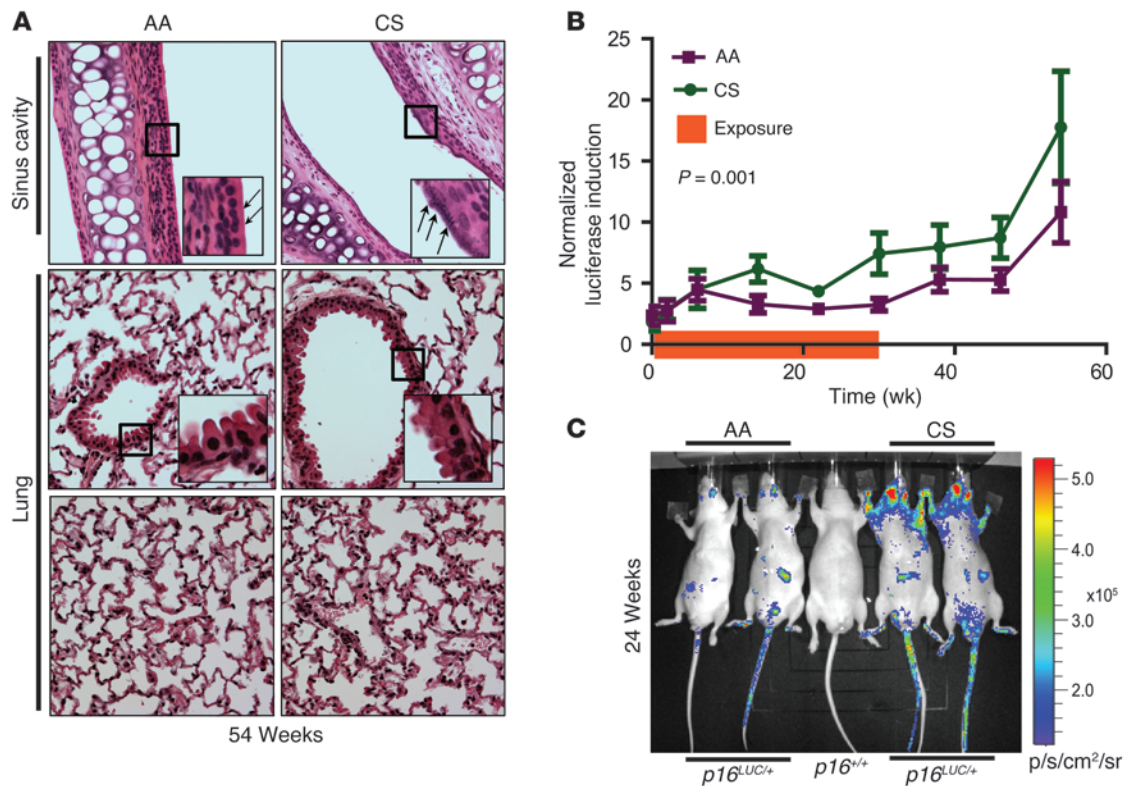
Figure 1
HFD does not increase *p16*[INK4a] expression, while arsenic moderately increases *p16*[INK4a] expression. *p16*[LUC] mice were (**A** and **B**) fed ND or HFD or (**C** and **D**) exposed to 0 or 50 ppm arsenic. (**A** and **C**) Luciferase intensity, normalized to mean luciferase levels of the entire cohort at day 0 and graphed as a function of time. Exposure duration is shown by the orange bar on the *x* axis. Error bars indicate SEM. *P* values were determined by linear regression analysis. (**B** and **D**) Representative TBLI of experiments in **A** and **C**, respectively.

spondingly, expression of *p16*[INK4a] mRNA was not altered in liver and spleen harvested from 18-month-old mice fed HFD versus ND (Supplemental Figure 1E). These data suggested that HFD does not accelerate *p16*[INK4a] expression in vivo, at least within the sensitivity of luciferase detection.

Arsenic is an environmental toxicant linked to human aging-associated phenotypes (i.e., several cancers, type II diabetes, and atherosclerosis; ref. 23). While not a direct clastogen, arsenic may indirectly affect DNA damage and repair (24–26). We examined the effect of chronic arsenic exposure on *p16*[INK4a] expression in vivo by administering 0 or 50 ppm arsenic to littermate *p16*[LUC] mice in the drinking water for 12 months starting at 8–10 weeks of age. After 48 weeks of exposure, arsenic-treated mice exhibited significant hepatic accumulation (Supplemental Figure 2A). Consistent with known effects of arsenic (27), treated mice showed small, structurally deranged pancreatic islets with an extreme decrease in total islet mass (Supplemental Figure 2, B and C). Overall survival rates were not different between cohorts (Supplemental Figure 2D). A mod-

est but significant increase in *p16*[INK4a] expression was observed by 24 weeks of exposure using TBLI (*P* = 0.023; Figure 1, C and D). Additionally, expression of *p16*[INK4a] mRNA was higher in spleen, but not liver, of 1-year-old mice administered 50 versus 0 ppm (Supplemental Figure 2E). These data suggest that chronic arsenic exposure modestly accelerates the accumulation of *p16*[INK4a]-expressing cells.

CS promotes DNA damage (28, 29) and age-related diseases such as emphysema, atherosclerosis, and several cancers (30, 31). Chronic CS exposure in humans is associated with increased *p16*[INK4a] expression in PBTLs (8, 32). To determine the effects of moderate CS exposure on cellular senescence in vivo, littermate *p16*[LUC] mice were exposed to CS or ambient air (AA) for 1 hour per day, 5 days per week for 6 months starting at 10–12 weeks of age. After 6 months of exposure, mice were further observed without CS up to 1 year of age. At the end of the study, histological analysis of the sinus cavity of CS-exposed mice showed particulate deposits along the epithelial layer of the nasal papilla, whereas no differences were noted in lung architecture between CS and AA cohorts at this tobacco dose (Figure 2A), which

Figure 2
CS increases *p16^INK4a* expression. *p16^LUC* mice were exposed to CS or AA. (**A**) Upper sinus cavity (top), airway bronchioles (middle; airway epithelium peg cells highlighted), and alveolar sacs (bottom) after 54 weeks. Arrows indicate areas of particulate deposit along the epithelial layer. Original magnification, ×40, ×280 (insets). (**B**) Luciferase intensity, normalized to mean luciferase levels of the entire cohort at day 0 and graphed as a function of time. Exposure duration is shown by the orange bar on the *x* axis. Error bars indicate SEM. *P* value was determined by linear regression analysis. (**C**) Representative TBLI of experiments in **B**.

was also not associated with accelerated mortality (Supplemental Figure 3A). A significant increase in *p16^INK4a* induction between the CS and AA cohorts, as measured by TBLI, was readily noted within weeks of CS exposure and persisted after CS was discontinued (Figure 2B). Consistent with histologic examinations of the nasal cavities and lungs (Figure 2A), luciferase induction was noted in the head and neck region of mice, but not the thoracic and abdominal regions (Figure 2C). Correspondingly, *p16^INK4a* mRNA levels in the liver, lung, axillary lymph nodes, and spleen were similar in CS- and AA-exposed mice (Supplemental Figure 3B). These data suggest that low-dose CS exposure accelerates accumulation of senescent cells in tissues that receive the highest exposure (i.e., nasal epithelium).

Chronic UVB exposure causes photoaging and skin cancer (33, 34). To directly assess whether chronic UVB induces senescence in vivo, the dorsal surface of *p16^LUC* mice was exposed to 350 J/m² UVB light 3 times a week for 6 months starting at 10–12 weeks of age. Littermate control mice were contemporaneously aged in the absence of UVB. After 6 months of exposure, mice were observed without further UVB exposure until 1 year of age. After 6 months of exposure, UV-exposed mice showed hyperkeratosis and metaplasia and inflammatory infiltration of the dermis and hypodermis compared with the nonexposed cohort (Figure 3A). The DNA damage marker phospho-H2AX was substantially increased in the epithelium of UV-exposed mice (Figure 3A and Supplemental Figure 4A), suggesting a persistent DNA damage response. Additionally, UV-exposed mice

developed skin neoplasms within 5 months of exposure, which accelerated mortality (Figure 3, B and C). Luciferase expression was higher in *p16^LUC* animals treated with UV than in unexposed controls prior to development of visible neoplasms, and TBLI was almost 8 times greater in UV-treated animals after 32 weeks of exposure (Figure 3D). In accord with the TBLI results (Figure 3E), *p16^INK4a* mRNA levels from abdominal and dorsal skin from both cohorts confirmed the site-specific induction of *p16^INK4a* expression (Figure 3F). Additionally, the UV-exposed dorsal skin exhibited higher expression than unexposed abdominal skin from the same mouse (Figure 3F).

To strengthen the association of *p16^INK4a* induction with senescence, additional markers were analyzed in UV-exposed and unexposed skin, including mRNA of the senescence-associated (SA) cytokines *Cxcl1* and *Il6* and SA-β-galactosidase (SA-β-gal) staining. *Cxcl1* and *Il6* expression increased in UV-exposed versus nonexposed mice. Additionally, increased expression only occurred in skin directly exposed to UV light (back) and not in unexposed skin (abdomen) from the same animals (Figure 3, G and H). We observed a similar pattern of SA-β-gal staining (Supplemental Figure 4B). These data suggest that chronic DNA damage from UV light accelerates senescent cell accumulation.

Here, we demonstrated that *p16^LUC* mice can detect the senescence-promoting effects of environmental exposures. Direct DNA-damaging agents (CS and UV light) appeared potently geronto-genic, and arsenic exposure produced a lesser, but significant, effect. We also identified anatomic gerontogenic effects of these
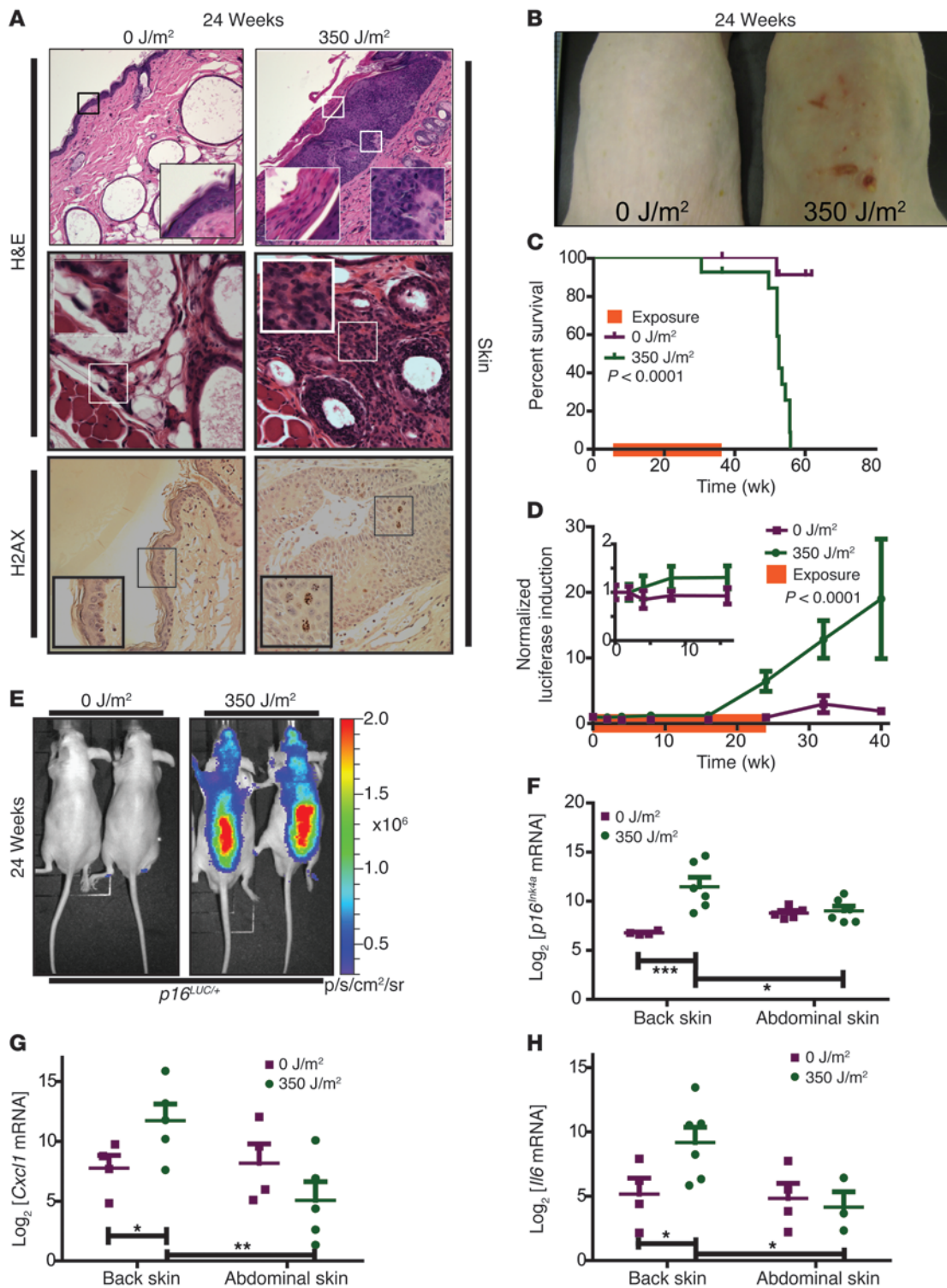
Figure 3
UVB increases $p16^{INK4a}$ expression. $p16^{LUC}$ mice were exposed to 0 J/m^2 ($n = 13$) or 350 J/m^2 ($n = 11$) UVB light. (**A**) Representative histopathological images of skin stained with H&E or phospho-H2AX. Original magnification, ×20 (top), ×40 (middle and bottom), ×200 (top, insets), ×120 (middle and bottom, insets). (**B**) Representative dorsal images. (**C**) Kaplan-Meier survival curves. Exposure duration is shown by the orange bar on the x axis. P value was determined by Gehan-Breslow-Wilcoxon test. (**D**) Luciferase intensity, normalized to mean levels of the entire cohort at day 0 and graphed as a function of time. Exposure duration is shown by the orange bar on the x axis. Inset highlights initial 20 weeks of exposure. Error bars denote SEM. P value was determined by linear regression analysis. (**E**) Representative TBLI of experiments in **D**. (**F**–**H**) Quantitative real-time PCR of $p16^{INK4a}$ (**F**), $Cxcl1$ (**G**), and $Il6$ (**H**) expression in back and abdominal skin at sacrifice. Error bars denote SEM. *$P < 0.05$, **$P < 0.01$, ***$P < 0.005$, Student's t test.

agents, including a stronger effect of passively inhaled CS on nasal epithelia than lung parenchyma (Figure 2C) and effects of UVB on exposed rather than unexposed skin (Figure 3, E and F).

This system has some important limitations. First, although luciferase imaging is considerably more sensitive than optical methods, the $p16^{LUC}$ allele may be less useful for detecting senescence in deeper organs or in rare cellular subtypes. Therefore, while we observed no effect of HFD on TBLI, it is possible that HFD activates senescence in important cellular compartments (e.g., pancreatic β cells, ref. 35; and vascular cells, refs. 21, 22), but not to a level detectable using this system. Similarly, while we showed that gerontogen-induced $p16^{INK4a}$ expression occurred spatially near senescent cells, we have not explicitly demonstrated that $p16^{INK4a}$-expressing cells are in all cases senescent. Finally, the $p16^{LUC}$ allele cannot be used to identify $p16^{INK4a}$-independent gerontogens or aging processes.

In summary, we demonstrated using modest-sized cohorts of serially analyzed animals that the $p16^{LUC}$ allele reported in vivo activation of senescence markers and uncovered gerontogenic effects of environmental toxicants. This resource can supplement other rodent platforms used for toxicological assessments; specifically, it represents an in vivo system with which to assess a compound's age-promoting activity. We believe this resource will provide an important tool for understanding the relationship between environmental exposures and molecular aging.

Methods

Further information can be found in Supplemental Methods.

Hairless SKH1-E $p16^{LUC/+}$ mice were used for all experiments (18). Genotyping was performed as previously described (18). For histologic analysis, tissues were fixed with 10% formalin overnight, then transferred to 70% ethanol for paraffin blocking and staining. Quantitative TaqMan RT-PCR strategies for detection of $p16^{INK4a}$ were performed as previously described (7, 13).

Statistics. Statistical significance was determined using 2-tailed Student's *t* test or linear regression analysis for all comparisons, except survival analysis (Gehan-Breslow-Wilcoxon test). A *P* value less than 0.05 was considered statistically significant.

Study approval. Experiments were performed under protocols approved by the University of North Carolina IACUC.

Address correspondence to: Norman E. Sharpless, The Lineberger Comprehensive Cancer Center, University of North Carolina School of Medicine, CB #7295, Chapel Hill, North Carolina 27599, USA. Phone: 919.966.1185; Fax: 919.966.8212; E-mail: nes@med.unc.edu.

1. Long GG, Morton D, Peters T, Short B, Skydsgaard M. Alternative mouse models for carcinogenicity assessment: industry use and issues with pathology interpretation. *Toxicol Pathol.* 2010;38(1):43–50.
2. Goldsworthy TL, et al. Transgenic animals in toxicology. *Fundam Appl Toxicol.* 1994;22(1):8–19.
3. Jacobson-Kram D, Sistare FD, Jacobs AC. Use of transgenic mice in carcinogenicity hazard assessment. *Toxicol Pathol.* 2004;32(suppl 1):49–52.
4. Martin GM. Interactions of aging and environmental agents: the gerontological perspective. *Prog Clin Biol Res.* 1987;228:25–80.
5. Nielsen GP, Stemmer-Rachamimov AO, Shaw J, Roy JE, Koh J, Louis DN. Immunohistochemical survey of p16INK4A expression in normal human adult and infant tissues. *Lab Invest.* 1999; 79(9):1137–1143.
6. Zindy F, Quelle DE, Roussel MF, Sherr CJ. Expression of the p16INK4a tumor suppressor versus other INK4 family members during mouse development and aging. *Oncogene.* 1997;15(2):203–211.
7. Krishnamurthy J, et al. Ink4a/Arf expression is a biomarker of aging. *J Clin Invest.* 2004;114(9):1299–1307.
8. Liu Y, et al. Expression of p16(INK4a) in peripheral blood T-cells is a biomarker of human aging. *Aging Cell.* 2009;8(4):439–448.
9. Molofsky AV, et al. Increasing p16INK4a expression decreases forebrain progenitors and neurogenesis during ageing. *Nature.* 2006;443(7110):448–452.
10. Janzen V, et al. Stem-cell ageing modified by the cyclin-dependent kinase inhibitor p16INK4a. *Nature.* 2006;443(7110):421–426.
11. Signer RA, Montecino-Rodriguez E, Witte ON, Dorshkind K. Aging and cancer resistance in lymphoid progenitors are linked processes conferred by p16Ink4a and Arf. *Genes Dev.* 2008;22(22):3115–3120.
12. Liu Y, et al. Expression of p16(INK4a) prevents cancer and promotes aging in lymphocytes. *Blood.* 2011; 117(12):3257–3267.
13. Krishnamurthy J, et al. p16INK4a induces an age-dependent decline in islet regenerative potential.

Nature. 2006;443(7110):453–457.
14. Jeck WR, Siebold AP, Sharpless NE. Review: a meta-analysis of GWAS and age-associated diseases. *Aging Cell.* 2012;11(5):727–731.
15. Berent-Maoz B, Montecino-Rodriguez E, Signer RA, Dorshkind K. Fibroblast growth factor-7 partially reverses murine thymocyte progenitor aging by repression of Ink4a. *Blood.* 2012;119(24):5715–5721.
16. Baker DJ, et al. Clearance of p16Ink4a-positive senescent cells delays ageing-associated disorders. *Nature.* 2011;479(7372):232–236.
17. Chen H, et al. PDGF signalling controls age-dependent proliferation in pancreatic beta-cells. *Nature.* 2011;478(7369):349–355.
18. Burd CE, et al. Monitoring tumorigenesis and senescence in vivo with a p16(INK4a)-luciferase model. *Cell.* 2013;152(1–2):340–351.
19. Burd CE, Jeck WR, Liu Y, Sanoff HK, Wang Z, Sharpless NE. Expression of linear and novel circular forms of an INK4/ARF-associated non-coding RNA correlates with atherosclerosis risk. *PLoS Genet.* 2010;6(12):e1001233.
20. Visel A, et al. Targeted deletion of the 9p21 non-coding coronary artery disease risk interval in mice. *Nature.* 2010;464(7287):409–412.
21. Wang CY, et al. Obesity increases vascular senescence and susceptibility to ischemic injury through chronic activation of Akt and mTOR. *Sci Signal.* 2009;2(62):ra11.
22. Shi Q, et al. Endothelial senescence after high-cholesterol, high-fat diet challenge in baboons. *Am J Physiol Heart Circ Physiol.* 2007;292(6):H2913–H2920.
23. Kapaj S, Peterson H, Liber K, Bhattacharya P. Human health effects from chronic arsenic poisoning--a review. *J Environ Sci Health A Tox Hazard Subst Environ Eng.* 2006;41(10):2399–2428.
24. Yamauchi H, Aminaka Y, Yoshida K, Sun G, Pi J, Waalkes MP. Evaluation of DNA damage in patients with arsenic poisoning: urinary 8-hydroxy-deoxyguanine. *Toxicol Appl Pharmacol.* 2004; 198(3):291–296.

25. Hartwig A, Groblinghoff UD, Beyersmann D, Natarajan AT, Filon R, Mullenders LH. Interaction of arsenic(III) with nucleotide excision repair in UV-irradiated human fibroblasts. *Carcinogenesis.* 1997; 18(2):399–405.
26. Andrew AS, Karagas MR, Hamilton JW. Decreased DNA repair gene expression among individuals exposed to arsenic in United States drinking water. *Int J Cancer.* 2003;104(3):263–268.
27. Paul DS, Harmon AW, Devesa V, Thomas DJ, Styblo M. Molecular mechanisms of the diabetogenic effects of arsenic: inhibition of insulin signaling by arsenite and methylarsonous acid. *Environ Health Perspect.* 2007;115(5):734–742.
28. DeMarini DM. Genotoxicity of tobacco smoke and tobacco smoke condensate: a review. *Mutat Res.* 2004; 567(2–3):447–474.
29. Pfeifer GP, Denissenko MF, Olivier M, Tretyakova N, Hecht SS, Hainaut P. Tobacco smoke carcinogens, DNA damage and p53 mutations in smoking-associated cancers. *Oncogene.* 2002; 21(48):7435–7451.
30. Bernhard D, Moser C, Backovic A, Wick G. Cigarette smoke — an aging accelerator? *Exp Gerontol.* 2007; 42(3):160–165.
31. Ito K, Barnes PJ. COPD as a disease of accelerated lung aging. *Chest.* 2009;135(1):173–180.
32. Nelson JA, et al. Expression of p16(INK4a) as a biomarker of T-cell aging in HIV-infected patients prior to and during antiretroviral therapy. *Aging Cell.* 2012;11(5):916–918.
33. Kligman LH. Photoaging. Manifestations, prevention, and treatment. *Clin Geriatr Med.* 1989; 5(1):235–251.
34. Scharffetter-Kochanek K, et al. Photoaging of the skin from phenotype to mechanisms. *Exp Gerontol.* 2000;35(3):307–316.
35. Sone H, Kagawa Y. Pancreatic β cell senescence contributes to the pathogenesis of type 2 diabetes in high-fat diet-induced diabetic mice. *Diabetologia.* 2005;48(1):58–67.